Applied Acoustics 114 (2016) 125–135

Contents lists available at ScienceDirect

Applied Acoustics

journal homepage: www.elsevier.com/locate/apacoust

Design and experimental tests of active control barriers for low-frequency stationary noise reduction in urban outdoor environment

Francesco Borchi [a,*], Monica Carfagni [a], Lorenzo Martelli [a], Alessio Turchi [a], Fabrizio Argenti [b]

[a] Dipartimento di Ingegneria Industriale, Università di Firenze, via Santa Marta, 3 – I-50139 Firenze, Italy
[b] Dipartimento di Ingegneria dell'Informazione, Università di Firenze, via Santa Marta, 3 – I-50139 Firenze, Italy

ARTICLE INFO

Article history:
Received 28 December 2015
Received in revised form 21 July 2016
Accepted 22 July 2016

Keywords:
Active noise control
Active-noise barrier
Low-frequency stationary noise
Urban noise

ABSTRACT

Active noise control (ANC) techniques are based on the emission of an antiphase signal in order to cancel the noise produced by a primary source. ANC has been successfully applied especially for reducing noise in confined environments, such as headphones and ducts. In this study, we present an application of ANC concepts to the design of an anti-noise barrier for an outdoor environment and its experimental testing. Even though passive techniques are effective in noise reduction at middle-high frequencies, they become less efficient at low frequencies (below 300 Hz) due to the limited dimensions of commonly deployable barriers. In this paper, we analyze the properties of a low-cost active noise system able to efficiently operate on stationary, almost pure-tone, low-frequency noise, such as that produced by electrical transformers and reactors in power and transformation plants. A prototype has been implemented and on-the-field experimental tests have been carried out. The results (confirmed also by numerical simulations) demonstrate a remarkable efficiency in the far field, with a reduction up to 15 dB with respect to the absence of the ANC system.

1. Introduction

Active noise control (ANC) techniques [1–3] are nowadays becoming more and more refined and have reached a high level of maturity that allowed their integration into modern acoustic devices, mainly targeted to hearing aids, headphones [4] and propagation of noise in ducts [5]. In recent years, applications proposed for an open field scenario (open spaces, ambient noise propagation [6,7]) also appeared. This latter field poses the most challenging problems, being subject to wind, rain, temperature gradients, randomly moving sources with broadband emission spectrum, etc.

One of the most promising research topics explored in this field in the last decade consists of the development of active noise barriers (ANB) able to perform active control of the noise propagated in the *shadow* zone through the diffraction over the barrier borders. In ANB applications, the ANC techniques may be coupled with passive ones for the reduction of broadband noise. Passive methods, based on noise absorbing and insulating materials, are effective in the mid-high frequency range of the audible spectrum, whereas their use at low frequencies (e.g., in the range 20–300 Hz) implies the deployment of high dimension barriers, depending on the wavelength to be canceled, which are unfeasible for economic and environmental impact reasons. On the other side, ANC techniques are able to implement a fairly good control of low-frequency noise emissions.

In recent years, a certain number of promising studies appeared in the literature, showing the feasibility of ANB solutions in the open field [6–18]. The key issue in ANB design is the availability of fast converging algorithms and filters in order to adapt to fast changing scenarios, either due to the variability of the noise signal to be canceled or to the environmental changes. Early theoretical studies of actively controlled noise barriers were reported by Omoto and Fujiwara [10] that studied the application of active noise control - and achieved cancellation of sound pressure - at the diffraction edge of the barrier. In the following decades, a relevant number of papers explored ANB solutions and produced important theoretical and experimental results. ANB prototypes were reported by Ohnishi et al. [6,11], showing the feasibility of a feedback active solution working with an artificial stationary broadband source, with an additional noise attenuation of about 4–5 dB (with respect to the passive barrier) in a region up to 10 m behind the barrier. Many theoretical studies explored advanced control methods [13,14] and refined the initially proposed techniques. In [16], an analog circuit feedback control system is used to deploy an active noise barrier, whereas in [17,18], the advantages of directional secondary sources are investigated.

* Corresponding author.
E-mail addresses: francesco.borchi@unifi.it (F. Borchi), monica.carfagni@unifi.it (M. Carfagni), fabrizio.argenti@unifi.it (F. Argenti).

http://dx.doi.org/10.1016/j.apacoust.2016.07.020
0003-682X/

Recently, the feasibility of an ANB solution with reductions of up to 10 dB in a controlled environment (anechoic room) has been demonstrated [7]. These results are promising if compared to the performance of passive anti-diffractive devices – usually placed on the top of the barrier - that allow an additional noise attenuation of only 1–2 dB with respect to a regular barrier to be achieved [19].

As to the features of possible noise sources in industrial contexts, there are plants and devices that produce almost-stationary low-frequency noise: one example is the case of electrical transformers and reactors in power generation and transformation plants. Even though such stations were originally built outside urban areas, as a consequence of urban expansion often they are now surrounded by residential buildings and the problem of noise reduction is relevant for people living in their neighborhood. Abating such type of noise by using only passive barriers, however, may be difficult. In the context of possible solutions for smart cities development, we present in this paper a technologically advanced ANB system aiming at reducing noise in the urban surroundings of power plants. The proposed solution uses the walls around the transformers of the power plant that are mandatorily deployed for safety reasons against accidental flames and fires. The dimensions of the walls, however, are not sufficient to cancel noise at low-frequencies. In this paper, we present the design of an ANC system for cancelling low-frequency stationary noise. The system uses the filtered-x least mean square (Fx-LMS) algorithm [1] to create the anti-noise signal that cancels out the primary source of noise. A testbed of the system, working in real-time, has been implemented and several experimental measurements to assess its performance have been performed. The results show that additional noise reduction (with respect to the absence of the ANC system) of more than 10 dB are achievable in the far field. The experimental results have been confirmed by computer simulations by using a finite element methods (FEM) software. Such simulations may also be useful to predict the system behavior in more general settings that were not covered by the experimental ones (an example is shown at the end of the paper).

The paper is organized as follows. In Section 2, the principle at the basis of the proposed ANC system is described. In Section 3, the control algorithm implemented in the prototype is presented. In Section 4, some computer simulations obtained by using a FEM software and aiming at investigating the influence of some geometrical parameters of the proposed system are shown. In Section 5, experimental results demonstrating the amount of noise attenuation experienced when the proposed ANC system is deployed are presented; some computer simulation results, to confirm the experimental ones, are shown as well. Some concluding remarks are given in Section 6.

2. Active noise control on a passive barrier

Noise control techniques, either active or passive, aim at minimizing the undesired noise, emitted from one or more *primary* sources, in a specific area of interest. The obvious solution is to act right at the primary noise sources, by developing more advanced devices (e.g., silent devices) or by enclosing them into a soundproof casing. This latter solution is often unfeasible due to physical constraints (e.g., heat dissipation), so that noise barriers became the main practical solutions applicable in the open field.

Noise barriers operate on the physical principle of diffraction that affects wave propagation through obstacle edges. Diffraction can be observed only if the relevant physical dimensions of the obstacle are at least comparable with that of the incident wavelength λ [20,21]. In the case of a barrier having height h, the requirement in order to have diffraction is $h > \lambda_{max}$, where λ_{max} is the largest wavelength present in the noise spectrum to be canceled. If the above condition is valid, the original noise signal is propagated in the shadow zone produced by the barrier mainly by diffraction (neglecting sound transmission through the barrier). The listener in the shadow zone is affected by "virtual" linear sources, generically denoted as P_{diff}, located over the barrier borders where diffraction takes place (see Fig. 1). An analytical model for P_{diff} is given by MacDonald [22,23] and it can be considered as a valid approximation if both source and listener are at a distance d much greater than λ_{max} from the border.

Since propagation analytical methods are quite complex, a general and practical technique for calculating the dimensions of a noise barrier can be retrieved from ISO 9613-2 (1996). This standard provides equations that allow the physical dimensions of a barrier to be correctly designed given the desired level of noise reduction at a specified position. In the case of a simple barrier with only one diffraction border the noise reduction Δ_b introduced by the barrier for each octave band of center wavelength λ, in the simplified version proposed in [24,25], is given by

$$\Delta_b = 10\log\left(3 + \frac{20}{\lambda}z\right)dB \tag{1}$$

where $z = r_1 + r_2 - r_d$ is the difference between the length of the indirect path ($r_1 + r_2$) and of the direct propagation path (r_d), as indicated in Fig. 1. In order to have a high efficiency, relevant z values - with respect to the wavelength - are necessary. This may be a critical point when low-frequency components dominate the noise spectrum and an arbitrarily high barrier cannot be deployed.

In order to combat noise in the shadow area and design a noise barrier working in the open field, ANC techniques can be thought as a valid solution - in combination with and complementary to passive ones – to obtain additional noise reduction mainly at low frequencies. In this specific case, we have the possibility to place the active control sources exactly on the border of the barrier, where also the virtual diffraction noise sources are localized. ANC systems work by emitting an antiphase signal that cancels out the undesired noise at specific points in space. In the case of a barrier with negligible noise transmission through the barrier, the listener in the shadow zone is affected only by the "virtual" diffraction source P_{diff}. By placing the ANC system right on the border of the barrier, since both control sources and "virtual" diffraction noise sources are spatially coincident, one can expect to completely control the propagation of noise in the whole shadow zone protected by the barrier, independently of the distance of the listener, obtaining a relevant noise reduction also in the far field.

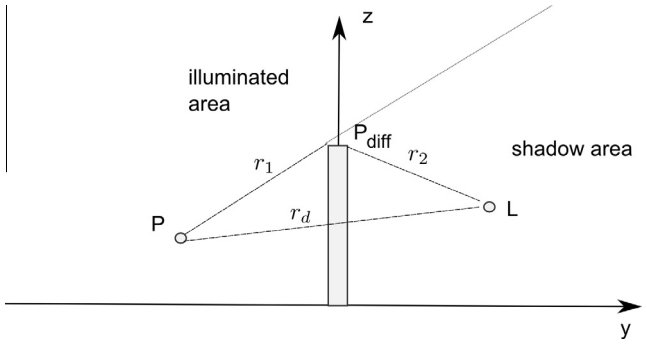

Fig. 1. A barrier divides the acoustic space into an "illuminated area", where the noise source have a direct acoustic path to a listener *L*, and a "shadow area", where noise is propagated through diffraction from the barrier border. The distance between the noise source *P* and the barrier edge and between the barrier edge and the listener L are denoted as r_1 and r_2, respectively, whereas r_d denotes the distance between *P* and *L*.

3. Control algorithm and prototype setup

In this work, we focused on the specific case of sources producing low-frequency noise, with approximately constant amplitude and with a principal component localized at 100 Hz, while the other components are negligible. This is the model of the noise produced by transformers and reactors in power and transformation plants, which stimulated this study. At these frequencies, a passive barrier should be extremely high: such a solution is deemed to be unfeasible for both economic and environmental impact reasons. On the other hand, walls are mandatorily built for safety reasons against accidental fires and flames propagation. Such walls are not sufficiently high to provide noise reduction for low-frequency noise, but they can represent the structure for supporting our ANC system.

The control algorithm that has been implemented is the multichannel adaptive filtered-x least mean square (Fx-LMS) [1,2], which is widely used for feed-forward ANC setups in many applications and shows a good performance for narrow-band low-frequency (<300 Hz) noise signals. Several versions of the Fx-LMS algorithm are available in the literature, e.g., the leaky Fx-LMS [26], that can be used to cope with numeric errors in finite-precision implementations, overloading of the secondary sources, and stability problems of the control loop. Stability problems may also arise due to the feedback from the secondary sources to the reference sensors. In this case, the feedback should be compensated in the controller [15]. Solutions for feedback neutralization based on feedback channel estimation are also discussed in [1]. In our experimental tests, employing the classical multichannel Fx-LMS algorithm, no stability problems were experienced. In the following, the Fx-LMS algorithm is summarized [3], with reference to Fig. 2 for the testbed layout and to Fig. 3 for the variables description.

Let N_R, N_C and N_E denote the number of reference microphones, number of control (or secondary) sources and number of error microphones, in that order. A set of N_RxN_C FIR adaptive filters, whose length is fixed and equal to J, are updated according to an LMS error criterion. Each filter is driven by a reference signal and controls a secondary source. The signal driving a single secondary source is obtained as

$$u_c[n] = \sum_{r=1}^{N_r} \boldsymbol{w}_{cr}^T[n]\boldsymbol{x}_r[n] \tag{2}$$

for $c = 1, 2, \ldots, N_c$, where $\boldsymbol{w}_{cr}[n] = [w_{cr,0}[n]\ w_{cr,1}[n]\ \ldots\ w_{cr,J-1}[n]]^T$ denotes the impulse response at time n of the filter driven by the rth reference signal and controlling the cth secondary source; $\boldsymbol{x}_r[n] = [x_r[n]\ x_r[n-1]\ \ldots\ x_r[n-J+1]]^T$ collects the last J samples of the rth reference signal. There are N_CxN_E secondary paths from the N_C secondary sources to the N_E error microphones: let $G_{ce}(z)$, $c = 1, 2, \ldots, N_c$, $e = 1, 2, \ldots, N_E$, denote the relative transfer functions and $\widehat{G}_{ce}(z)$ an estimation of these functions. Then, the updating rule according to the multi-channel Fx-LMS algorithm is given by

$$\boldsymbol{w}_{cr}[n+1] = \boldsymbol{w}_{cr}[n] + \mu\sum_{e=1}^{N_E} \boldsymbol{x}'_{rce}[n]\varepsilon_e[n] \tag{3}$$

where

$$\boldsymbol{x}'_{rce}[n] = \hat{g}_{ce}[n] * \boldsymbol{x}_r[n] \tag{4}$$

with $\hat{g}_{ce}[n]$ denoting the estimated secondary path impulse response, $\varepsilon_e[n]$, $e = 1, 2, \ldots, N_E$, the error signals, and $*$ the convolution of two sequences. In Eq. (3), μ represents an adaptation step, which is a critical parameter for convergence speed and accuracy. Even though this value can be chosen adaptively [27,28], experimental results have shown that a constant μ is sufficiently adequate for our goals.

The multi-channel Fx-LMS algorithm has been described in a general setting, with an arbitrary number of reference microphones, secondary sources and error microphones. In the actual implementation of our prototype, we used a number of error microphones equal to the number of control sources, i.e., $N_E = N_C$. Each error microphone was placed in front of the cone of one control source and in close proximity to the diffraction border of the barrier. The number of reference microphones was also chosen equal to the number of control sources, i.e., $N_R = N_C$. Each reference microphone was placed between the primary and one of the secondary sources (see Fig. 2), in proximity of the latter. Thus, from a physical standpoint, a reference and an error microphone are structurally coupled to a single secondary source; from an algorithmic standpoint, however, the whole set of error signals contributes to updating all adaptive filters coefficients, as ruled by (3), whereas the whole set of reference signals contributes to build all the control signals, as specified in (2). The secondary sources are placed at a distance d_L by each other, with $d_L < \lambda/2$ [10], in order to produce an efficient noise cancellation. The control apparatus was placed on the illuminated side of the barrier, where the noise source is located, at a distance from the primary source greater than the noise wavelength λ.

The details of the prototype configuration and the instrumentation used for its implementation are given in Section 5.

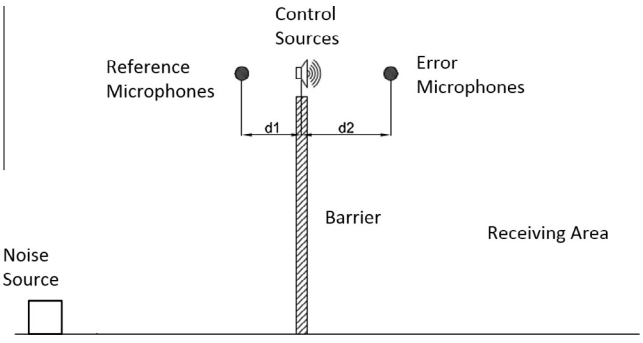

Fig. 2. Testbed layout.

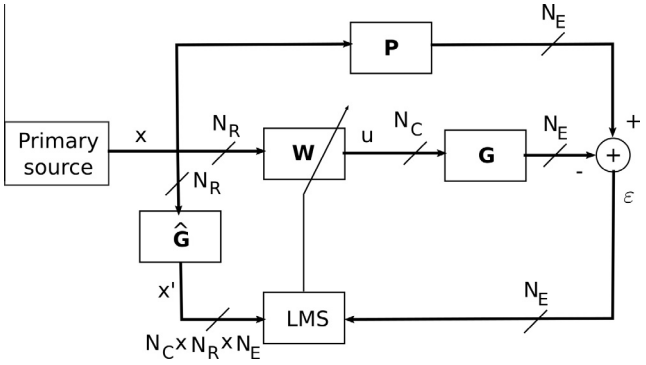

Fig. 3. Fx-LMS scheme. **P** and **G** denote the primary and secondary paths; $\widehat{G}$ is an estimation of **G**; **W** indicates the set of adaptive filters whose updating is ruled by the LMS algorithm.

4. Analysis of secondary sources geometrical configuration by means of FEM simulations

Before proceeding with on-the-field experiments, some simulations were performed in order to analyze the geometrical

configuration of the secondary sources. The FEM software Comsol Multiphysics was used.

A simplified scenario was simulated, in which a single border of a barrier is covered by the ANC system. The ANC system is composed by an array of secondary sources and an array of error microphones, the latter placed on the barrier edge. We assumed that the number of error microphones was equal to the number of control sources and that each error microphone was placed in front of a control source at a given distance. A single primary point source is located on the same side of the ANC system. Details can be seen in Fig. 4 (top left). The simulations space is a quadrant of a cylinder of radius 16 m and height 10 m. The barrier is 10 m high and 7.5 m wide. The ground is perfectly reflecting, while all other boundaries are assumed as acoustically perfect absorbent to represent a free

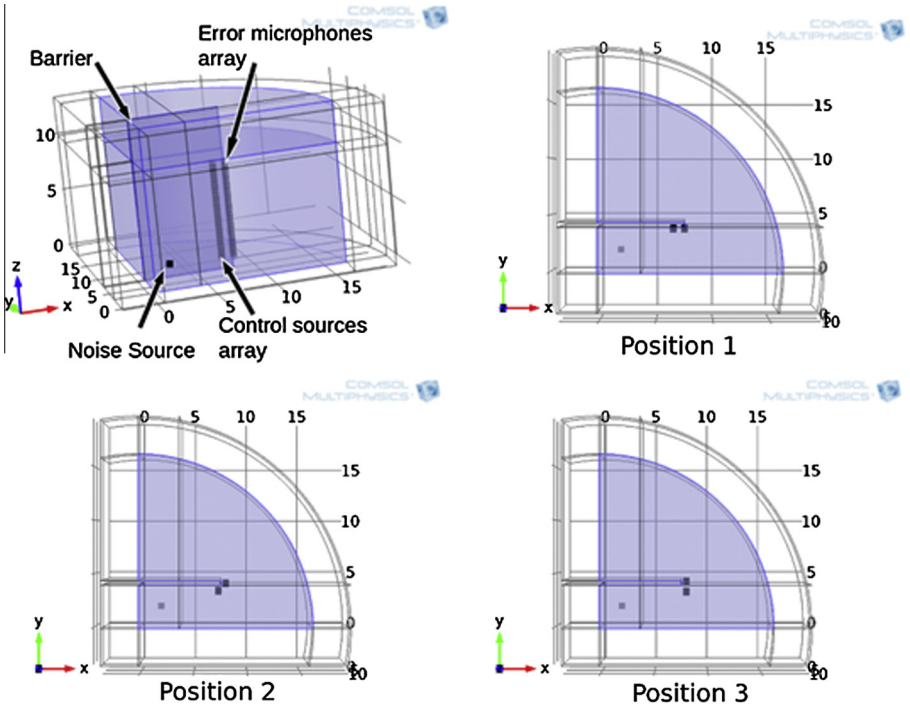

Fig. 4. Simplified scenario used in numerical simulations with Comsol Multiphysics. Positions 1–3 refer to the three different alignment of control sources/error microphones arrays that were tested.

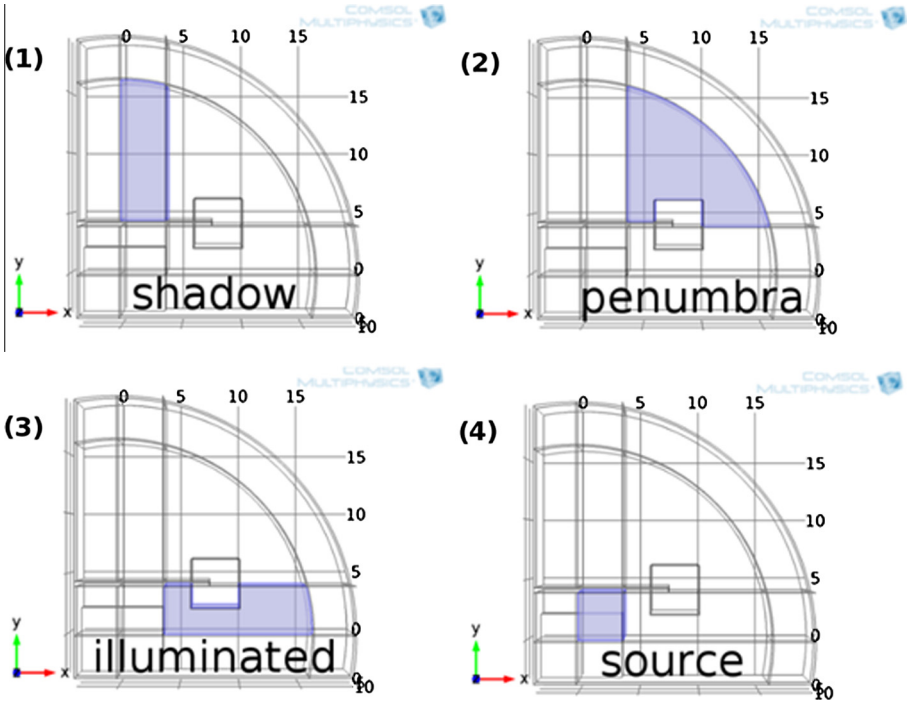

Fig. 5. Definition of the volumes used to evaluate average sound pressure level. The white square (of side 3 m and centered on the error microphones), was excluded from averages calculation in order to remove near-field effects.

field propagation. The noise source emits a 100 Hz pure tone signal and is positioned at 1.7 m from the simulation borders, 2.3 m from the barrier.

The objective of the simulations was testing the performance of the ANC system vs. the distance between the control sources and the distance between the control sources array and the error microphones array; three different alignments of the axis between the secondary sources and error microphones arrays were also tested, i.e., by positioning these elements parallel, at 45° and orthogonal to the barrier, as sketched in Fig. 4 top-right, bottom-left and bottom-right and denoted as Positions 1, 2, and 3, in that order. Due to numerical constraints to perform simulations, only the peak performance of the system is simulated, that is the system is supposed to act at convergence of the Fx-LMS algorithm. In other words, control sources are considered as point-like and their emission is tuned in amplitude and phase in order to produce a signal that minimizes the pressure levels on the error microphones.

In order to evaluate the average noise attenuation produced by the ANC system, four different volumes, as depicted in Fig. 5, were defined. The "shadow" zone is where the noise emission from the primary source is expected to be shadowed; the "illuminated" zone is where the receiver is in line-of-sight of the source; the "penumbra" zone is an intermediate area where we expect fringes of interference and performance degradations; the "source" zone is in proximity of the primary source, i.e., where we expect to have reflections from the barrier. Performances are evaluated by taking the average pressure level in the above defined volumes. The average noise reduction is computed as the difference between the average sound pressure levels obtained with and without the ANC system active.

A first set of outcomes of the simulations are shown in Fig. 6. By using the configuration labelled as "Position 1", the distance between each control source was varied (thus, the number of control sources to cover the whole border varies as well). The distance between the control sources array and the error microphones array was set to 1 m. As can be seen from Fig. 6(a), a rapid decrease of the performance of the ANC system in the shadow area (the one of interest for us) is experienced when the distance between the control sources becomes larger than one half of the wavelength, whereas the performance loss is almost negligible for smaller distances. In Fig. 6(b), the distance between the control sources array and the error microphones array was varied, whereas the distance between control sources was set to 1 m. As can be seen, performances do not degrade too much for distances longer than 1 m.

As a final test, we compared the ANC performance with respect to the three geometrical configurations denoted as Positions 1, 2 and 3, previously defined. The results, shown in Fig. 7, demonstrate that the most efficient configuration is the one labelled as "Position 1", i.e., with the axis between the secondary sources and error microphones arrays parallel to the barrier. We extended this test by considering a spatially extended noise source (3.5 m square base and 2 m tall), placed on the ground and centered on the

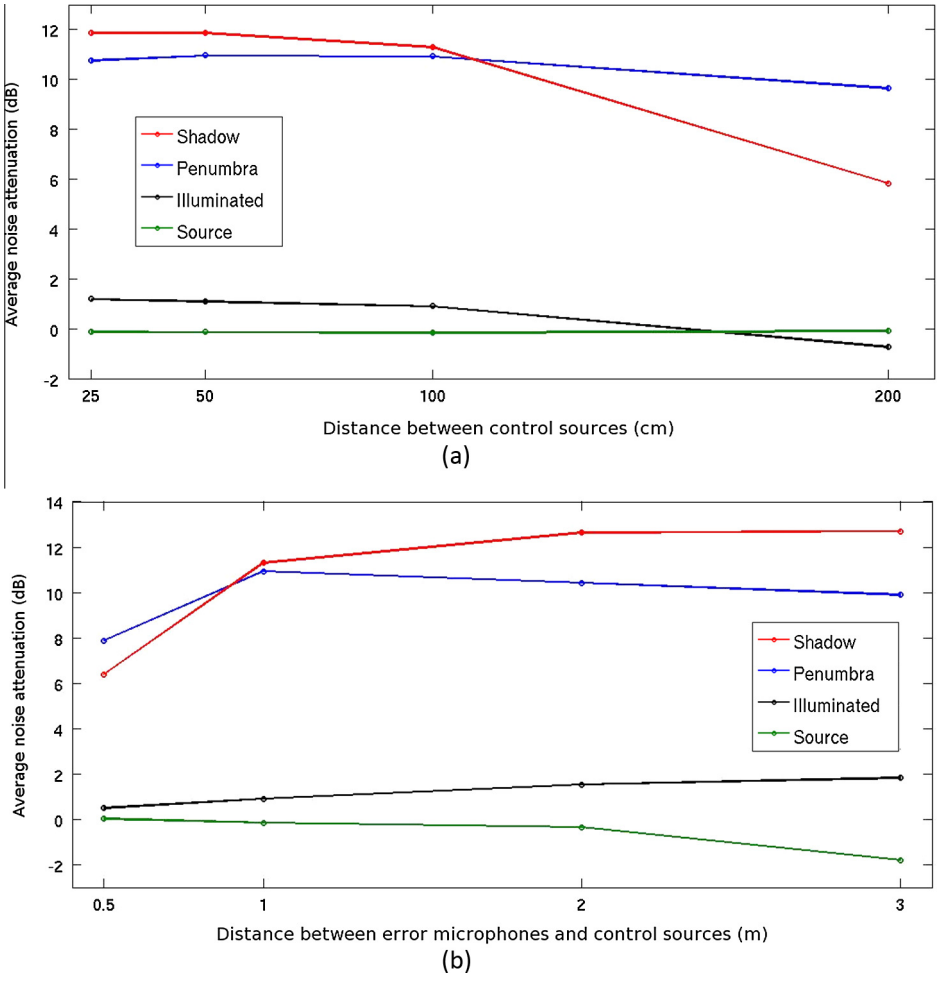

Fig. 6. Performance of the ANC system in each zone depending on different ANC configurations: (a) average noise attenuation vs. the distance between the control sources (distance between control sources array and error microphones array set to 1 m); (b) average noise attenuation vs. the distance between control sources array and error microphones array (distance between control sources set to 1 m).

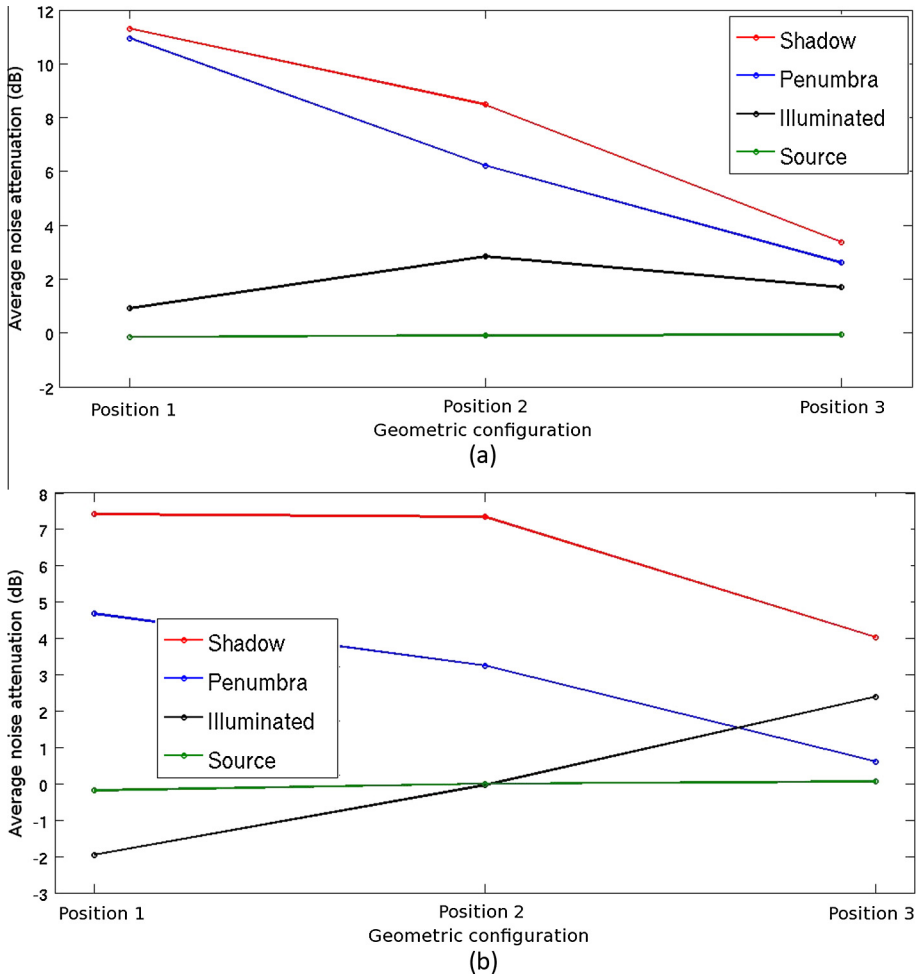

Fig. 7. Performance of the ANC system in each zone depending on the deployed geometrical configuration: (a) point-like noise source; (b) spatially extended noise source.

position of the previous point-like source. In this latter case, we observe that the performance loss is much reduced, especially concerning the shadow zone, so that also "Position 2" becomes a viable solution.

5. Experimental results

The prototype has been tested in an operating environment mimicking the border of a barrier and, successively, on one border of a true rectangular barrier deployed close to a reactor in an electricity power plant. In both cases, computer simulations were also performed to confirm the measured noise attenuations and the obtained results are shown as well.

5.1. Prototype configuration and instrumentation

The prototype has been implemented by using the following instrumentation:

- Error and reference microphones: Behringer ECM8000.
- Preamplifiers: eight channel Presonus Digimax FS.
- ADC-DAC board: sixteen channel Lynx Aurora 16, 24 bit/sample, sampling frequency 44,100 Hz.
- Loudspeakers: K-Array loudspeakers, mounting 7 in. B&C Speakers cones.
- Amplifier: Powersoft Ottocanali 1204.

Fig. 8. Deployment of the ANC system at the corner of a building.

- Personal computer/audio board: 4-core CPU @3.40 GHz, RAM 16 GB, audio board RME HDSPe MADI FX.

Other details of the software and digital signal processing implementation are the following:

- the multi-channel Fx-LMS algorithm was implemented in Matlab, integrated with routines in C for most burdensome steps;
- since the signals have a band much lower than the acquisition sampling frequency, in order to reduce the computational burden, the Fx-LMS algorithm worked in a decimated domain. A decimation factor equal to 8 was used; the length of the FIR lowpass filters used to downsample reference and error signals (and to upsample the control signals before digital-to-analog conversion) was set to 32 coefficients;
- the length of the Fx-LMS adaptive filters was set to 60 coefficients;
- the secondary path was modeled as a simple delay, whose value depends on the distance between the secondary source and the error microphone;
- in order to make the system more robust to external interferences, a bandpass filter (implemented in the digital domain as a fourth order elliptic filter, with cutoff frequencies 60 Hz and 150 Hz) was applied to the reference and error signals.

5.2. First experimental tests: building corner

In the first experiments, we used the corner edge of a high building, as shown in Fig. 8. This setup allowed to demonstrate the performance of the system in the presence of a single diffraction border largely covered by the ANC system. Fig. 9 shows a top view scheme of the deployment, in which the positions of the elements that compose the system (below detailed) are sketched.

In this configuration, the primary noise source is represented by a loudspeaker generating a 100 Hz pure tone. It is placed at a distance $d_1 = 2\ \lambda$ from the corner and $d_2 = \lambda/2$ from the wall, being $\lambda = 3.43$ m. The secondary sources are placed in the illuminated area as well, so that the control signals encounter the same diffraction phenomenon as the primary one. The error microphones are in

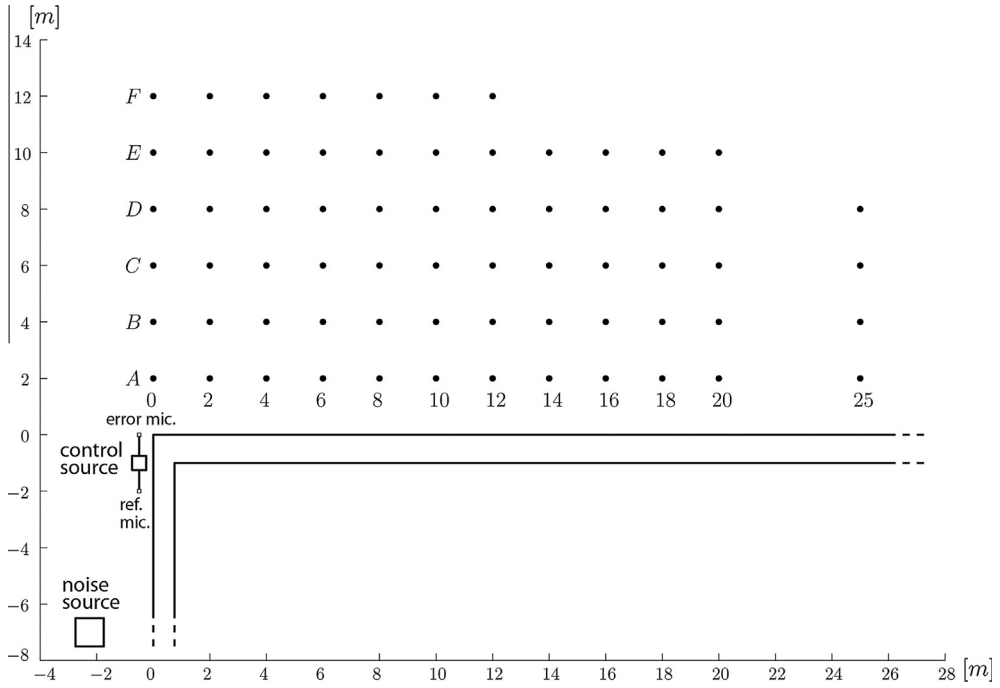

Fig. 9. Top view of the first experimental setting. The noise source is placed on one side of the corner and the error microphones in proximity of the corner edge. The dots indicate the measurement points.

Table 1
Sound pressure levels in dB (third octave band centered at 100 Hz frequency) measured on the grid points showed in Fig. 9. For each entry, on the left the values with the ANC system switched off, on the right the gain in noise reduction (when negative) introduced by its activation.

Points	A	B	C	D	E	F
0	92.4 (−5.6)	90.0 (−4.5)	85.5 (−8.0)	81.8 (−7.4)	84.3 (−9.3)	85.8 (−6.8)
2	89.0 (−7.7)	83.2 (−1.5)	78.0 (−0.3)	81.5 (−15.0)	80.3 (−6.5)	83.0 (−11.5)
4	83.6 (−18.6)	74.0 (+2.2)	76.7 (−12.7)	81.6 (−17.1)	82.0 (−11.6)	81.5 (−5.9)
6	77.0 (−7.0)	75.3 (−11.3)	79.3 (−5.0)	77.8 (−3.3)	78.2 (−4.0)	75.7 (−6.4)
8	83.8 (−5.1)	81.0 (−5.8)	78.8 (−11.6)	76.3 (−12.3)	72.8 (−2.1)	73.4 (−0.6)
10	77.8 (−9.0)	78.8 (−3.4)	80.2 (−4.6)	76.1 (−4.6)	73.5 (−6.3)	73.0 (−12.0)
12	66.0 (+2.4)	75.0 (−9.2)	74.5 (−9.3)	76.0 (−6.8)	78.3 (−6.5)	76.8 (−10.0)
14	77.8 (−9.6)	70.0 (−4.9)	65.6 (−10.7)	76.2 (−12.5)	78.4 (−6.7)	
16	78.5 (−6.7)	76.3 (−6.5)	73.4 (−13.9)	72.5 (−15.4)	71.0 (−1.1)	
18	79.4 (−16.1)	77.3 (−13.4)	65.7 (−0.8)	76.5 (−7.6)	78.7 (−4.8)	
20	74.4 (−11.2)	71.3 (−6.5)	70.0 (−8.9)	72.4 (−3.1)	72.9 (+1.9)	
25	78.5 (−14.7)	71.3 (−4.9)	76.1 (−8.7)	72.6 (−13.7)		

proximity of the corner edge. In the shadowed area, noise attenuation is expected and measured as described below.

The setup included six secondary sources placed at a vertical distance between each other of 70 cm. As already mentioned in Section 3, a reference and an error microphone were structurally assembled together with each single secondary source loudspeaker, even though all error and reference signals contribute to build the control signals, as specified by Eqs. (2) and (3). The error microphones were placed 65 cm away from the cone of each transducer and the same distance was used between the reference microphones and the secondary sources. The elements were mounted vertically in order to have the error microphones aligned with the corner edge, at a distance of 40 cm from it. The total height of the corner edge covered by the ANC system was 4.2 m from the ground; even though the coverage of the corner is only partial, relevant noise reduction in the shadowed area has been measured.

Noise reduction has been evaluated by measuring the noise levels when the ANC system is switched off and after its activation. The grid of measurement points is shown in Fig. 9; the height of each measurement point from the ground was 1.7 m. As can be seen, the area covered by the grid is tenth of meters wide. In Table 1, the noise levels in dB, measured in the third octave band centered at 100 Hz, are shown as well as the noise attenuation (expressed as a negative gain) introduced by the activation of the ANC system. From these results, it can be seen that the performance, in terms of noise attenuation, does not significantly decrease with distance, even though the presence of interference patterns causes the noise reduction not to be uniform. The spatial average noise attenuation, taken over all the measurement points, introduced by the activation of the ANC system is 7.6 dB, with a peak of about 15 dB measured 25 m away from the building corner. Causes of performance degradation include a partial coverage with control sources of the building diffraction edge as well as the wind, which induces oscillations on the structure used to raise the system along the corner. In Fig. 10, a sample error signal, measured at one of the error microphones, is shown, demonstrating the stability of the algorithm and the relatively fast convergence (less than 1 s) compatible with our specific target application where the noise is assumed as stationary.

A computer simulation obtained with Comsol Multiphysics, aiming at confirming the experimental results obtained on-the-field, is shown in Fig. 11, where the gain in noise reduction, computed at 1.7 m from the ground, is mapped. Noise attenuation values in accordance to those obtained experimentally and reported in Table 1 were achieved. In particular, the spatial average noise attenuation in the dashed rectangular area depicted in Fig. 11 (enclosing, approximately, the measurement points depicted in

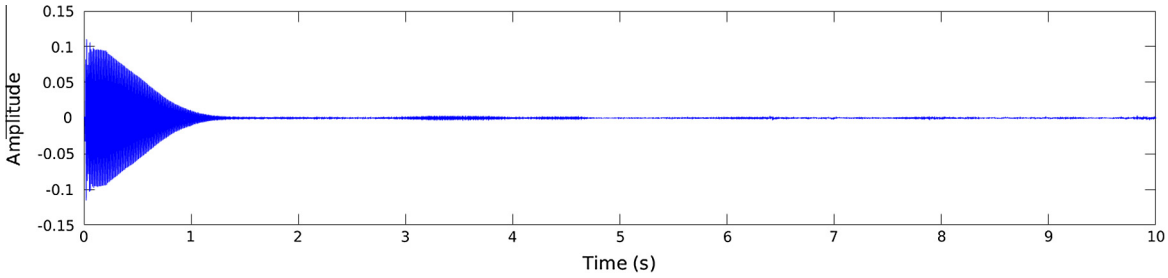

Fig. 10. Signal levels of the fourth (from the ground) error microphone. A similar behavior is encountered for all microphones. Amplitude is directly proportional to the measured pressure level.

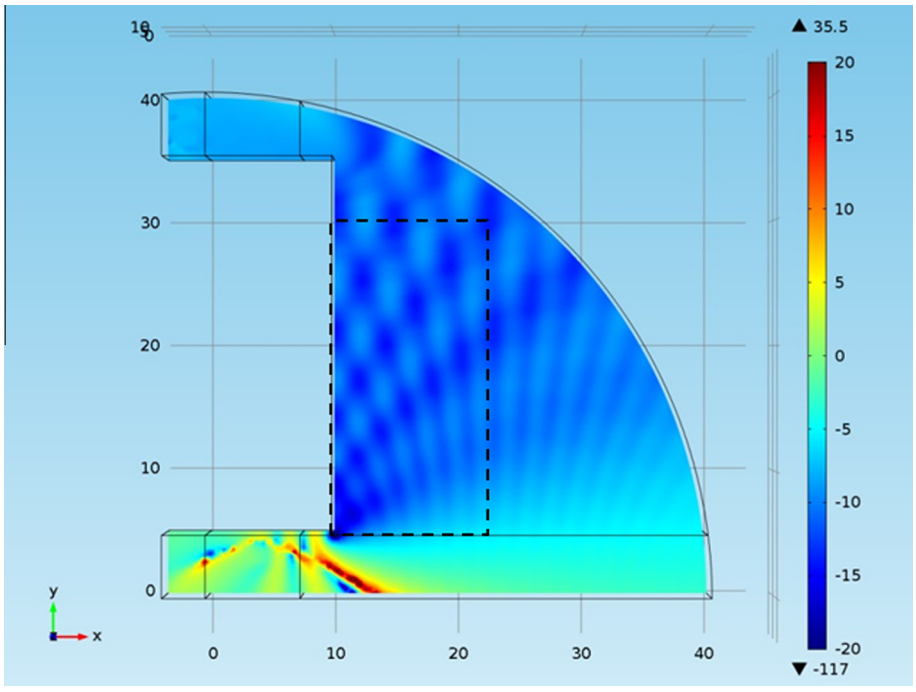

Fig. 11. Noise gain (in dB) after the activation of the ANC system (at 1.7 m from the ground): numerical simulation of a scenario similar to the first experimental tests setting.

Fig. 12. Deployment of the ANC system at an electricity generation station in Tuscany (Italy).

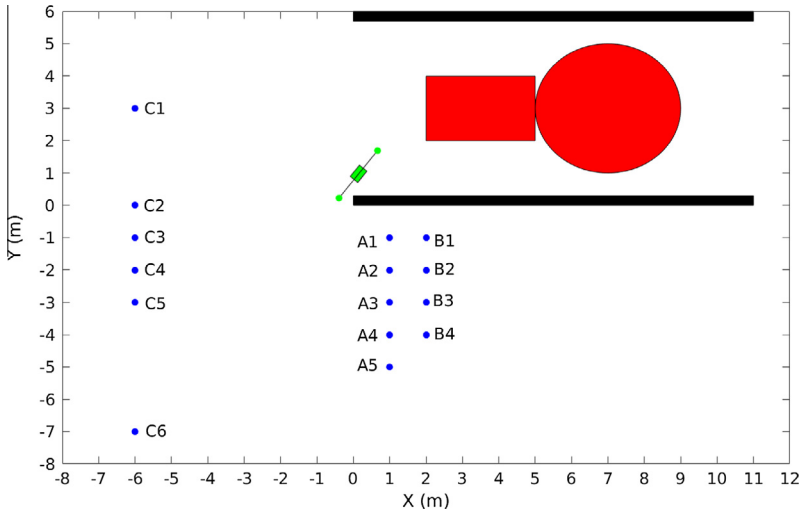

Fig. 13. Top view of the second experimental setting. The noise source is placed on one side of the barrier, the ANC system close to one of the lateral borders. The dots indicate the measurement points.

Fig. 9) is 9.6 dB. The fulfilment of ideal conditions in the simulation tests (e.g., no presence of wind, system tuned to achieve zero pressure levels at the error microphones, as discussed for the simulations in Section 4) explains the obtained higher average attenuation value.

5.3. Second experimental tests: barrier

In the second experiments, the system was mounted on a barrier deployed (for safety reasons against fire and flames) close to a reactor of an electricity power plant in Tuscany (Italy). The deployment of the system is shown in Fig. 12. In this setup, only one of the possible diffraction borders of the barrier is partially covered by the ANC system. In Fig. 13, a top view of this second experimental setting is sketched.

The configuration of the ANC system was similar to the one of the first experiment. This time, only five secondary sources were used and the length of the border they covered was only 3.5 m; the barrier height was 9 m, but the presence of high voltage cables prevented us from achieving a higher coverage. As to the alignment of the control sources/error microphones arrays, "Position 2" (see Section 4) was the only one allowed by the infrastructure of the plant. As in the previous tests, noise reduction was evaluated by measuring the noise levels when the ANC system is switched off and after its activation. The grid of measurement points is shown in Fig. 13. Sound pressure levels (in dB, measured in the third octave band centered at 100 Hz) with the ANC system switched off and the difference introduced by its activation are shown in Table 2.

As can be seen, apart from few points, noise reduction is still experienced, even though the effectiveness of the ANC system is reduced with respect to the first experiments. This is assumed to be due to the limitedness of the coverage of the diffraction borders (some simulation results considering a larger coverage are discussed in Section 5.4).

Table 2
Sound pressure levels in dB (third octave band centered at 100 Hz frequency) measured on the grid points showed in Fig. 13. For each entry, on the left the values with the ANC system switched off, on the right the gain in noise reduction (when negative) introduced by its activation.

Points	1	2	3	4	5	6
A	58 (−8)	65 (−6)	70 (−4)	69 (−2,5)	68 (+1)	
B	68 (−2)	64 (−1)	67 (0)	65 (+3)		
C	73 (−2)	72 (−2)	63 (−3)	65 (−2)	69 (−1,5)	73 (−1)

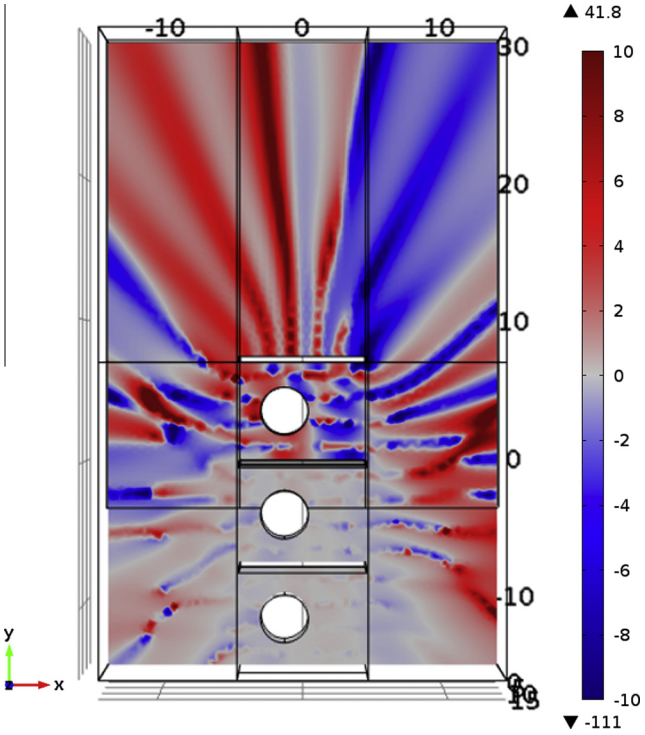

Fig. 14. Noise gain (in dB) after the activation of the ANC system (at 1.5 m from the ground): numerical simulation of a scenario similar to the second experimental tests setting.

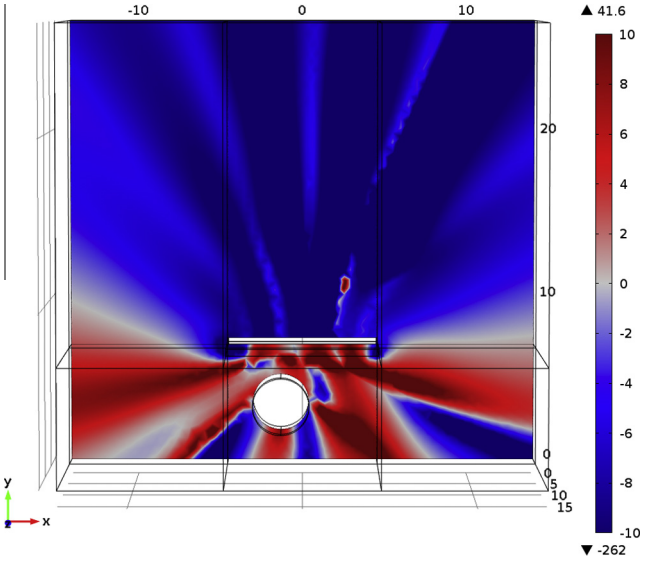

Fig. 15. Noise gain (in dB) after the activation of the ANC system (at 1.5 m from the ground): numerical simulation of a scenario with all the borders of the barrier covered by the ANC system.

The experimental results achieved on-the-field have been confirmed by computer simulations obtained by using Comsol Multiphysics. In Fig. 14, we report the gain in noise reduction computed in a scenario mimicking the ANC configuration deployed at the power plant, where three reactors separated by barriers are present. The primary sources were simulated as cylindrical noise sources and an ANC system, composed of five secondary sources, was placed on the edge of the topmost barrier. As can be seen, the simulated values are compatible with those reported in Table 2.

5.4. Further simulation results

In order to predict the performance of the ANC system in the case the perimeter of the barrier were fully covered by control sources, some (only simulation) results were further produced. A simplified scenario with respect to that in Fig. 14 was simulated. A single barrier, 9 m high and 9 m wide, was considered. The control sources were positioned along the whole perimeter of the barrier at a distance of 1 m each other. The distance between control sources and error microphones was set to 1 m. The primary noise source was simulated as a cylindrical reactor (radius 2 m and height 5 m), emitting a pure tone noise signal at 100 Hz. In Fig. 15, the simulated noise reduction (at 1.5 m from the ground) is shown. As can be seen, an average sound pressure level attenuation of about 8–10 dB in a wide area beyond the barrier (shadow area) is experienced.

6. Conclusions

In this paper, a low-cost ANB solution, using commercially available audio equipment and standard PC control hardware, has been implemented and tested. The objective was to control the noise propagated through diffraction over a barrier border. The solution is targeted to continuous-cycle stationary noise sources emitting low-frequency tone-like noise, e.g., transformers and reactors of an electricity generation power plant. Preliminary experimental tests and numerical simulations showed the feasibility of the proposed active control solution and noticeable performance in the far field, with an average spatial attenuation of more than 7 dB and peak attenuations of 15 dB and over. The preliminary prototype solution developed in this work is simple and uses a limited number of secondary sources. A considerable improvement of the performances is expected with an advanced system acting over all the diffraction borders of the barrier, whose implementation, however, should address several challenging issues. First, if the number of secondary loudspeakers is high, a modular realization of the system must be devised in order to achieve a computationally feasible solution. Each module will still be a multichannel system, with inter-module as well as (adjacent) inter-module error feedback. Even though the classical multichannel Fx-LMS algorithm worked fairly well and no stability problems were experimentally encountered when dealing with the stationary noise taken into consideration in this paper, more refined versions, e.g., [26], of the basic algorithm may be tested. Another interesting technique, which may be included for performance

improvements as well as to facilitate the physical structure implementation, is the concept of virtual microphone control [29–31]. Virtual microphones signals are not acquired by actual sensors but are synthesized by using physical microphones acquisitions located close to the control system. An adaptive algorithm works to minimize the noise in the remote locations where the virtual microphones are simulated. Such methods have been proposed in several applications where the distance between physical and virtual microphones is short (of the order of tens of centimeters), but also for ANC barriers where such a distance is much longer [15].

Acknowledgments

This work was supported by the Electroacoustic Engineering Laboratory (INEA Lab) of Florence University and by the "Ente Cassa Risparmio" of Florence (Italy). The authors would like also to thank TERNA (Italian grid operator for electricity transmission) for allowing the on-the-field experimental tests in the power plant. The authors wish also to thank the anonymous reviewers for their constructive comments that helped them to improve the quality of the original submission.

References

[1] Kuo SM, Morgan DR. Active noise control systems. Hoboken (NJ): John Wiley & Sons; 1996.
[2] Elliott SJ. Signal processing for active control. 1st ed. Academic Press; 2001.
[3] Kuo SM, Morgan DR. Active noise control: a tutorial review. Proc IEEE 1999;87(6):943–73.
[4] Rudzyn B, Fisher M. Performance of personal active noise reduction devices. Appl Acoust 2012;73(11):1159–67.
[5] Bai MR, Zeung P. Implementation of a broadband duct ANC system using adaptive spatially Feedforward structure. J Sound Vib 2002;251(5):891–903.
[6] Ohnishi K, Saito T, Teranishi S, Namikawa Y, Mori T, Kimura K, et al. Development of the product-type active soft edge noise barrier. In: Proceedings of the 18th international congress on acoustics, Kyoto, Japan. p. 1041–4.
[7] Jung TH, Kim JH, Kim KJ, Nam SW. Active noise reduction system using multi-channel ANC. In: 11th International Conference on Control, Automation and Systems (ICCAS). p. 36–9.
[8] Omoto A, Takashima K, Fujiwara K, Aoki M, Shimizu Y. Active suppression of sound diffracted by a barrier: an outdoor experiment. J Acoust Soc Am 1997;102(3):1671–9.
[9] Zou H, Lu J, Qiu X. The active noise barrier with decentralized Feedforward control system. In: 17th International Congress on Sound & Vibration, Cairo, Egypt, 18–22 July, 2010.
[10] Omoto A, Fujiwara K. A study of an actively controlled noise barrier. J Acoust Soc Am 1993;94(4):2173–80.
[11] Ohnishi K, Teranishi S, Nishimura M, Uesaka K, Hachimine K, Ohnishi H. Development of the noise barrier using active controlled acoustical soft edge. In: Proc of ACTIVE99. p. 595–606.
[12] Nagamatsu H, Ise S, Shikano K. Numerical study of active noise barrier based on the boundary surface control principle. Proc of Active 1999;99:585–94.
[13] Nakashima T, Ise S. Active noise barrier for far field noise reduction. In: Proceedings of the 18th international congress on acoustics, Kyoto, Japan.
[14] Hasebe M, Yamanishi T. Active control of the sound field diffracted by a noise barrier. In: Proceedings of the 18th international congress on acoustics, Kyoto, Japan.
[15] Berkhoff AP. Control strategies for active noise barriers using near-field error sensing. J Acoust Soc Am 2005;118(3):1469–79.
[16] Liu JC, Niu F. Study on the analogy feedback active soft edge noise barrier. Appl Acoust 2008;69(8):728–32.
[17] Chen W, Pu H, Qiu X. A compound secondary source for active noise radiation control. Appl Acoust 2010;71(2):101–6.
[18] Chen W, Rao W, Min H, Qiu X. An active noise barrier with unidirectional secondary sources. Appl Acoust 2011;72(12):969–74.
[19] May DN, Osman MM. The performance of sound absorptive, reflective, and T-profile noise barriers in Toronto. J Sound Vib 1980;71(1):65–71.
[20] Maekawa Z. Noise reduction by screens. Appl Acoust 1968;1(3):157–73.
[21] Kurze UJ, Anderson GS. Sound attenuation by barriers. Appl Acoust Jan. 1971;4(1):35–53.
[22] MacDonald HM. A class of diffraction problems. Proc Lond Math Soc 1915;14(1):410–27.
[23] Isei T, Embleton TFW, Piercy JE. Noise reduction by barriers on finite impedance ground. J Acoust Soc Am 1980;67:46–58.
[24] Moreland JB, Musa RS. The performance of acoustic barriers. In: International Conference on Noise Control Engineering, Washington D.C.. p. 95–104.
[25] Tatge RB. Noise reduction of barrier walls. In: Arden House Conference.
[26] Tobias OJ, Seara R. Leaky-FXLMS algorithm: stochastic analysis for Gaussian data and secondary path modeling error. IEEE Trans Speech Audio Process 2005;13(6):1217–30.
[27] Ardekani IT, Abdulla WH. Study of convergence behavior of real-time adaptive active noise control systems. In: Proceedings of the second APSIPA annual summit and conference, Singapore. p. 534–7.
[28] Babu P, Krishnan A. A new variable threshold and dynamic step size based active noise control system for improving performance. Int J Comput Sci Inform Sec 2010;7(2):160–5.
[29] Petersen CD. Optimal spatially fixed and moving virtual sensing algorithms for local active noise control Ph.D. thesis. South Australia: School of Mechanical Engineering, The University of Adelaide; 2007.
[30] Pawelczyk M. Noise control in the active headrest based on estimated residual signals at virtual microphones. In: Proc. 10th international congress on sound and vibration, Stockholm, Sweden.
[31] Pawelczyk M. A two-stage wiener filter based multi-channel feedback virtual microphone acoustic noise reducing system. Arch Acoust 2007;32(4):917–22.